

The Effect of Surfaces on the Tunneling Density of States of an Anisotropically Paired Superconductor

L.J. Buchholtz

Department of Physics, California State University, Chico, Chico, CA 95929, USA

Mario Palumbo, D. Rainer

Physikalisches Institut, Universität Bayreuth, D-95440 Bayreuth, Germany

J.A. Sauls

Department of Physics & Astronomy, Northwestern University, Evanston, IL 60208, USA

Abstract

We present calculations of the tunneling density of states in an anisotropically paired superconductor for two different sample geometries: a semi-infinite system with a single specular wall, and a slab of finite thickness and infinite lateral extent. In both cases we are interested in the effects of surface pair breaking on the tunneling spectrum. We take the stable bulk phase to be of $d_{x^2-y^2}$ symmetry. Our calculations are performed within two different band structure environments: an isotropic cylindrical Fermi surface with a bulk order parameter of the form $\Delta \sim k_x^2 - k_y^2$, and a nontrivial tight-binding Fermi surface with the order parameter structure coming from an anti-ferromagnetic spin-fluctuation model. In each case we find additional structures in the energy spectrum coming from the surface layer. These structures are sensitive to the orientation of the surface with respect to the crystal lattice, and have their origins in the detailed form of the momentum and spatial dependence of the order parameter. By means of tunneling spectroscopy, one can obtain information on both the anisotropy of the energy gap, $|\Delta(\mathbf{p})|$, as well as on the phase of the order parameter, $\Delta(\mathbf{p}) = |\Delta(\mathbf{p})|e^{i\varphi(\mathbf{p})}$.

To appear in J. Low Temp. Phys., Vol. 101, Dec., 1995

I. INTRODUCTION

In this paper we study the density of states spectrum of a d -wave superconductor in the vicinity of a specularly reflecting surface. The anomalous spectral properties of anisotropic superconductors and superfluids have been discussed in several publications [1–12]. The present work logically follows our examination of the system's order parameter and surface free energy which was presented in Ref. [13] (from here on we refer to this paper simply as [I]). Together, these studies are part of an ongoing effort to systematically examine measurable features which are typical of d -wave superconductors. We hope, as before, to contribute to the fund of theory necessary for their definitive experimental identification.

As discussed in [I], one expects that an anisotropic order parameter will respond strongly to pair-breaking effects near a wall which is, again, why we have chosen this setting as our arena of study. Moreover, the resulting spectrum of excitation states is quite sensitive to the details of the entire system and is also accessible to a variety of experimental probes. Accordingly, there are any number of spectral dependencies one could examine which may well yield significant clues as to the true symmetry of the order parameter. We have chosen three for this paper: 1) surface to lattice orientation, 2) realistic Fermi-surface geometries, and 3) finite size effects. The results presented here are not in any way intended as exhaustive studies of any of these areas. Instead, we selected out of a rather large collection of calculations a condensed subset which we felt was either representative of general behavior or exceptionally suggestive of potential experimental verification.

We employ the quasiclassical formulation of superconductivity for the calculations of this paper and refer the reader to [I] for a more detailed discussion of these methods. The equations of particular importance for the current work are collected in section II, and the results are displayed in the two subsections of section III. In section IV we discuss various aspects of the physical significance of our resulting data and we conclude with a summary of the most prominent points.

II. QUASICLASSICAL THEORY

A. Basic Equations

In [I] we presented the fundamental equations of the quasiclassical theory in the imaginary-energy (Matsubara) representation. These considerations provide a sufficient framework for the study of the thermodynamic properties of the system. A discussion of the spectral properties of the system, however, requires the real-energy version of the Green function equations presented in [I]. We therefore must compute the retarded propagator, \hat{g}^R , which can be defined in terms of the Matsubara propagator as follows (see, for example, Ref. [14]):

$$\hat{g}^R(\mathbf{p}_f, \mathbf{R}; \epsilon) = \hat{g}(\mathbf{p}_f, \mathbf{R}; \epsilon_n) \Big|_{i\epsilon_n \rightarrow \epsilon + i\eta}. \quad (1)$$

The 2×2 matrix propagator \hat{g}^R obeys a transport equation of the same form as in the case of imaginary energies:

$$\left[\epsilon \hat{\tau}_3 - \hat{\Delta}(\mathbf{p}_f, \mathbf{R}), \hat{g}^R(\mathbf{p}_f, \mathbf{R}; \epsilon) \right] + i \mathbf{v}_f(\mathbf{p}_f) \cdot \vec{\nabla}_{\mathbf{R}} \hat{g}^R(\mathbf{p}_f, \mathbf{R}; \epsilon) = 0, \quad (2)$$

with the same normalization condition,

$$[\hat{g}^R(\mathbf{p}_f, \mathbf{R}; \epsilon)]^2 = -\pi^2 \hat{1}. \quad (3)$$

Here $\mathbf{v}_f(\mathbf{p}_f)$ is the momentum dependent Fermi velocity, and $\hat{\Delta}(\mathbf{p}_f, \mathbf{R})$ is the superconducting order parameter (or pairing self-energy). For anisotropic superconductors $\hat{\Delta}(\mathbf{p}_f, \mathbf{R})$ exhibits, in general, a nontrivial dependence on the momentum, \mathbf{p}_f , and the position, \mathbf{R} , which must be calculated self-consistently from the gap-equation. The method for carrying out the self-consistent solution for $\hat{\Delta}$ was discussed in detail in [I] and will not be repeated here. Instead, we simply carry over the results obtained in [I] for the self-consistent order parameter and use them as input in the solution of equations (2) and (3) for \hat{g}^R .

The propagator \hat{g}^R carries detailed information on the quasiparticle excitations. In the quasiclassical scheme, a quasiparticle state is characterized by its excitation energy, ϵ , measured from the Fermi energy, and by a Fermi surface coordinate, \mathbf{p}_f , which is the projection of the quasiparticle momentum onto the Fermi surface. The total number of quasiparticle states (per spin) with energy, ϵ , in the energy interval $d\epsilon$, and Fermi momentum, \mathbf{p}_f , in the interval $d\mathbf{p}_f$ is given by

$$dN(\mathbf{p}_f, \mathbf{R}; \epsilon) = N_f n(\mathbf{p}_f) \nu(\mathbf{p}_f, \mathbf{R}; \epsilon) d\mathbf{p}_f d\epsilon, \quad (4)$$

where N_f is the total density of states in the normal state as measured, for example, by specific heat experiments. Band-structure effects lead to the anisotropy factor $n(\mathbf{p}_f)$, which is normalized such that $\oint d\mathbf{p}_f n(\mathbf{p}_f) = 1$. Finally, the effects of superconductivity on the density of states are carried by the dimensionless quantity $\nu(\mathbf{p}_f, \mathbf{R}; \epsilon)$,

$$\nu(\mathbf{p}_f, \mathbf{R}; \epsilon) = -\frac{1}{2\pi} \Im \left\{ \text{Tr} \left[\hat{\tau}_3 \hat{g}^R(\mathbf{p}_f, \mathbf{R}; \epsilon) \right] \right\}, \quad (5)$$

which we refer to in the remainder of the text as the “superconducting DOS factor”. In the normal state, $\nu(\mathbf{p}_f, \mathbf{R}; \epsilon) = 1$. In what follows we focus on the calculation of the quantity $\nu(\mathbf{p}_f, \mathbf{R}; \epsilon)$, and, in particular, how its qualitative features are affected by the presence of a wall.

We consider two different sample geometries: a semi-infinite system occupying the space $x > 0$, and a slab of finite thickness, w , and infinite lateral extent oriented perpendicular to the x -axis. In both cases we consider perfectly reflecting (specular) walls. Continuity of the propagator along a classical trajectory requires [15,16]:

$$\hat{g}^R(\mathbf{p}_{f,\text{in}}, \mathbf{R}_{\text{wall}}; \epsilon) = \hat{g}^R(\mathbf{p}_{f,\text{out}}, \mathbf{R}_{\text{wall}}; \epsilon), \quad (6)$$

which yields the appropriate quasiclassical boundary condition for a specular wall. An in-coming trajectory is defined as one in which $\mathbf{v}_f(\mathbf{p}_{f,\text{in}}) \cdot \hat{n} < 0$ while an out-going trajectory requires that $\mathbf{v}_f(\mathbf{p}_{f,\text{out}}) \cdot \hat{n} > 0$ (here \hat{n} is taken to be the surface normal pointing into the sample). The out-going momentum vector, $\mathbf{p}_{f,\text{out}}$, is then given in terms of the in-coming momentum vector, $\mathbf{p}_{f,\text{in}}$, by requiring that the momentum component parallel to the surface be conserved upon reflection,

$$\mathbf{p}_{f,\text{out}}^{\parallel} = \mathbf{p}_{f,\text{in}}^{\parallel}. \quad (7)$$

Note that energy conservation is implied in equation (6) since $\epsilon_{\text{in}} = \epsilon_{\text{out}}$.

We restrict our attention to the case of simple Fermi surfaces in which any given “in-coming” trajectory is *uniquely* connected to an “out-going” trajectory via equation (7). This boundary condition would need to be modified for systems with more complicated Fermi surfaces (e.g. multiple Fermi sheets, etc.), and additional phenomenological parameters would be required to determine the probability of a given in-coming trajectory being reflected into any one of the multiple out-going channels.

B. Nontrivial Band-structure

Before the self-consistent order parameter can be calculated and a complete solution of equation (2) can be carried out, we must first specify the form of the Fermi surface, the corresponding Fermi velocity, $\mathbf{v}_f(\mathbf{p}_f)$, the anisotropy factor, $n(\mathbf{p}_f)$, and the quasiparticle pairing interaction, $V(\mathbf{p}_f, \mathbf{p}'_f)$ (see equation (4) in [I]). We approach this problem in two different ways. First we consider an isotropic cylindrical Fermi surface with a pairing interaction that can be parameterized in terms of simple trigonometric functions (as in [I]). The second approach, which we carry over from Refs. [17] and [18], is to use actual tight-binding fits to the band-structure of high- T_c materials, along with a pairing interaction derived from a microscopic spin-fluctuation theory. The first of these two approaches was discussed in detail in [I], and we therefore focus on the second approach in what follows.

Following Radtke and Norman [18], we approximate the band-structure of the high- T_c cuprate superconductors by a 2d tight-binding model of the form:

$$E(\mathbf{p}) = t_0 + \frac{t_1}{2} [\cos p_x + \cos p_y] + t_2 \cos p_x \cos p_y + \frac{t_3}{2} [\cos 2p_x + \cos 2p_y] + \frac{t_4}{2} [\cos 2p_x \cos p_y + \cos 2p_y \cos p_x] + t_5 \cos 2p_x \cos 2p_y. \quad (8)$$

Given a Fermi energy, E_f , we use the relations $E_f = E(\mathbf{p}_f)$ and $\mathbf{v}_f = \vec{\nabla}_{\mathbf{p}} E(\mathbf{p})|_{E_f}$ to extract the Fermi wavevector, \mathbf{p}_f , at every point on the Fermi surface, along with the corresponding Fermi velocity, $\mathbf{v}_f(\mathbf{p}_f)$. These quantities then allow us to compute the anisotropy factor, $n(\mathbf{p}_f)$, in the usual way. Once the band structure data is known, the pairing interaction kernel can be evaluated using the weak-coupling version of the spin-fluctuation model of Radtke *et. al.* [17] as follows:

$$V(\mathbf{p}_f, \mathbf{p}'_f) = -V_0^* F(\mathbf{p}_f - \mathbf{p}'_f), \quad (9)$$

where

$$F(\mathbf{q}) = \left[\frac{1}{1 + J_0(\cos q_x a + \cos q_y a)} \right]^2. \quad (10)$$

One obtains this weak-coupling version of the interaction presented in Ref. [17] by integrating-out the high-energy degrees of freedom [14]. In doing so one introduces a cutoff, ϵ_{co} , and a renormalized interaction parameter, V_0^* , which differs, in general, from the bare interaction parameter of Ref. [17]. The renormalized interaction strength, together with the energy cut-off, can always be eliminated in favor of the superconducting transition temperature, T_c . Hence our pairing interaction is determined by two phenomenological parameters: the transition temperature, T_c , and the exchange coupling parameter, J_0 . The transition temperature is written in terms of the energy cut-off (in the weak-coupling theory) via:

$$T_{c\mu} = 1.13\epsilon_{co}e^{-1/\lambda_\mu} \quad (11)$$

where the λ_μ are dimensionless coupling constants in the various symmetry channels (see below).

Once the quasiparticle pairing interaction is known, the superconducting order parameter can be computed by self-consistently solving the weak-coupling gap equation (equation (4) in [I]) in the Matsubara representation. This equation can be recast into a more convenient form by introducing a complete set of eigenvalues and eigenfunctions of the interaction kernel:

$$\lambda_\mu \eta_\mu(\mathbf{p}_f) = \oint d\mathbf{p}'_f n(\mathbf{p}'_f) V(\mathbf{p}_f, \mathbf{p}'_f) \eta_\mu(\mathbf{p}'_f), \quad (12)$$

where the eigenfunctions, $\eta_\mu(\mathbf{p}_f)$, satisfy the orthonormality condition:

$$\oint d\mathbf{p}_f n(\mathbf{p}_f) \eta_\mu(\mathbf{p}_f) \eta_\nu^*(\mathbf{p}_f) = \delta_{\mu\nu}. \quad (13)$$

If we now express the superconducting order parameter as a linear combination of these eigenfunctions,

$$\hat{\Delta}(\mathbf{p}_f, \mathbf{R}) = \sum_{\mu} \hat{\Delta}_{\mu}(\mathbf{R}) \eta_{\mu}(\mathbf{p}_f), \quad (14)$$

then the gap equation may be rewritten as a series of equations for the individual gap amplitudes as follows:

$$\hat{\Delta}_{\mu}(\mathbf{R}) = \lambda_{\mu} T \sum_{\epsilon_n}^{\epsilon_{co}} \oint d\mathbf{p}_f n(\mathbf{p}_f) \eta_{\mu}^*(\mathbf{p}_f) \hat{f}(\mathbf{p}_f, \mathbf{R}; \epsilon_n). \quad (15)$$

The eigenfunction, $\eta_{\mu}(\mathbf{p}_f)$, associated with the largest (attractive) eigenvalue λ_{μ} determines the symmetry of the bulk stable phase, at least near T_c . We assume that this symmetry persists to all temperatures. The effects of the other symmetry components however (whether they are associated with attractive or repulsive eigenvalues), may become noticeable in the vicinity of surfaces [13], defects, in the cores of vortices, etc.

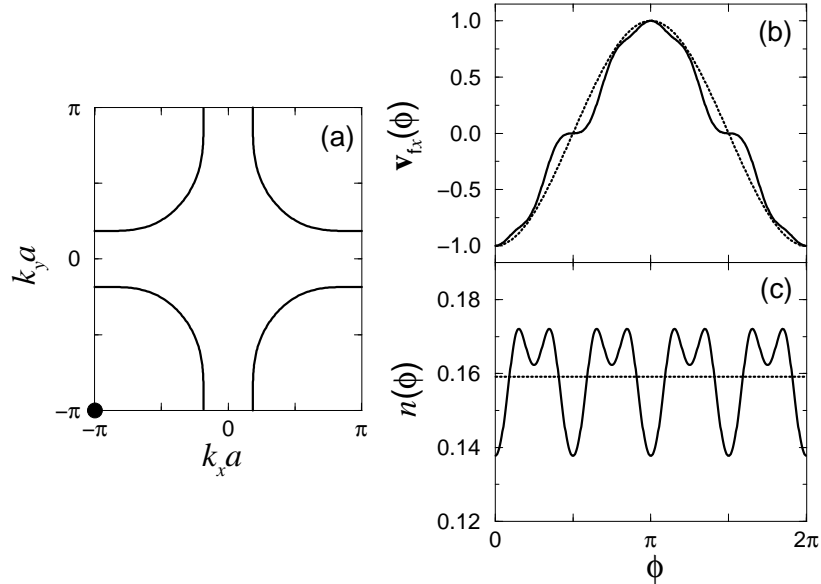


Fig. 1. Band-structure data: (a) The Fermi surface in the first Brillouin zone. We parameterize this surface by an angle $\phi = [0, 2\pi]$ taking the point indicated by the solid dot as the origin. In the repeated zone scheme our Fermi surface is then a single continuous line, around the origin, which is single-valued in ϕ . (b) The x -component of the Fermi velocity normalized so that the maximum is 1. (c) The anisotropy factor of the normal state density of states. The dotted lines show the corresponding values for the isotropic cylindrical Fermi surface.

In practice, equation (15) must be solved numerically, which first requires the numerical evaluation of the eigenvalues, λ_{μ} , and eigenfunctions, $\eta_{\mu}(\mathbf{p}_f)$, as defined in equation (12). Since we would like to expand our order parameter in terms of eigenfunctions of well defined symmetry, we first project out the pieces of the interaction matrix, $V(\mathbf{p}_f, \mathbf{p}'_f)$, which transform like each of the four one dimensional representations of the D_{4h} (tetragonal) group (i.e. $V_{A_1}(\mathbf{p}_f, \mathbf{p}'_f)$, $V_{A_2}(\mathbf{p}_f, \mathbf{p}'_f)$, $V_{B_1}(\mathbf{p}_f, \mathbf{p}'_f)$, $V_{B_2}(\mathbf{p}_f, \mathbf{p}'_f)$). We then use each of these matrices in place of the $V(\mathbf{p}_f, \mathbf{p}'_f)$ in equation (12) to solve for the eigenvalues and eigenfunctions corresponding to each symmetry classification. These eigenfunctions then allow us to construct a gap consisting of specific symmetry components, while the eigenvalues give the coupling strengths in the various symmetry channels.

We calculate the Fermi surface data using the parameter values reported in Ref. [17] for the YBCO(2,bf) sample (i.e. $t_0 = 0.0, t_1 = -1.0, t_2 = 0.38, t_3 = -0.09, t_4 = 0.0, t_5 = 0.0$, all in units of eV). The Van Hove singularity for this

system lies at about $E = -.46eV$ [19], and we take a Fermi energy slightly above this value at $E_f = -.30eV$. The resulting form of the Fermi surface in momentum space is shown in Fig. 1a. Repeating the Brillouin zone (repeated zone scheme) allows us to parameterize our Fermi surface by a polar angle ϕ around the $\mathbf{k} = (-\pi/2, -\pi/2)$ point in the Brillouin zone (denoted by a solid black dot in Fig. 1a). In Figs. 1b and 1c we plot the Fermi velocity, $\mathbf{v}_f(\phi)$, and the normalized density of states anisotropy factor, $n(\phi)$, as functions of ϕ . The factor $n(\phi)$ is obtained from equation (4), yielding

$$N_f n(\phi) d\phi = \frac{1}{(2\pi)^2} \frac{[\mathbf{p}_f(\phi)]^2}{|\mathbf{p}_f(\phi) \cdot \mathbf{v}_f(\phi)|} d\phi, \quad (16)$$

and is normalized such that $\int_0^{2\pi} d\phi n(\phi) = 1$.

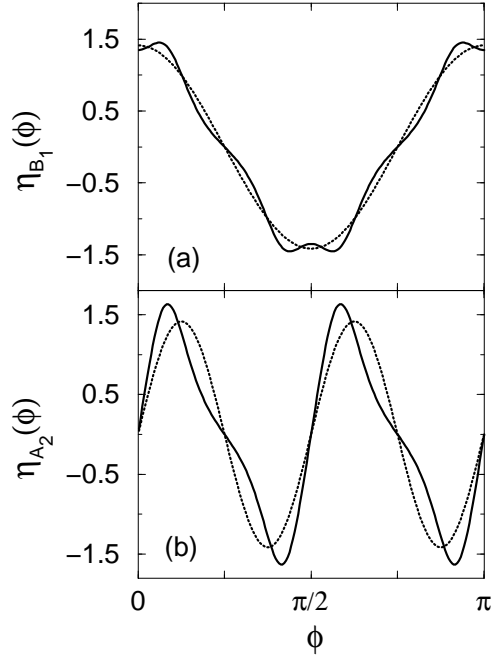


Fig. 2. The momentum space dependence of the B_1 and A_2 order parameter components as computed from the weak-coupling spin-fluctuation model discussed in section II-B. The dotted lines show the corresponding results when a cylindrical Fermi surface is used.

Once the band-structure data is known, we may then proceed to compute the spin-fluctuation pairing interaction via equation (9). Choosing the dimensionless parameters $V_0^* = -1.0$ and $J_0 = 0.4$, we find two attractive symmetry channels: B_1 and A_2 . The B_1 channel has the highest transition temperature while the A_2 channel has a T_c that is reduced by about 3/7 (the transition temperatures for the repulsive symmetry channels are set to zero in what follows). Within the dominant symmetry channel, the next to leading coupling constant is more than two orders of magnitude smaller than the leading coupling constant and therefore only the leading contribution is considered. The angular distribution of the order parameter components corresponding to the B_1 and A_2 symmetry channels are depicted in Figs. 2a and 2b.

III. RESULTS

We consider in both of the following subsections a surface geometry of the same form as in [I]. The normal to the surface is taken to lie along the \hat{x} -axis, which need not, in general, be parallel to the crystal lattice basis vector \hat{a} , from which we measure all our angles. We denote the angle between \hat{a} and the surface normal, \hat{x} , by ϕ_o , and the angle between \hat{a} and the momentum of an out-going trajectory, $\mathbf{p}_{f,\text{out}}$, by ϕ . This geometry is represented graphically in Fig. 1 of [I]. We denote the transition temperature for the bulk symmetry channel (B_1) by T_c while the transition

temperatures for the other symmetry channels are denoted explicitly by T_{cA_1} , T_{cA_2} , T_{cB_2} . All length scales are measured in units of the coherence length which we define in the usual way by $\xi = \hbar|\mathbf{v}_f|_{max}/\pi\Delta_{max-bulk}$.

A. Semi-Infinite System

We consider a semi-infinite system occupying the space $x > 0$ with a perfectly reflecting (specular) wall located at $x = 0$. The order parameter and free energy of this system were calculated in detail in [I] (considering an ideal cylindrical Fermi surface) for several different symmetry parameterizations of the order parameter. From our calculations of these quantities in the case of the tight-binding band-structure and spin-fluctuation pairing interaction discussed in section II-B, we conclude that the thermodynamic properties of this system are quite insensitive to the details of the Fermi surface geometry, as long as the band-structure does not become too pathological. Hence, we do not discuss the stability of the self-consistent order parameter calculations here. Instead, we use these results to calculate \hat{g}^R from equation (2), and then focus our attention on the excitation spectrum. This includes the response of the excitation spectrum to an admixture of subdominant components and to nontrivial band-structure effects.

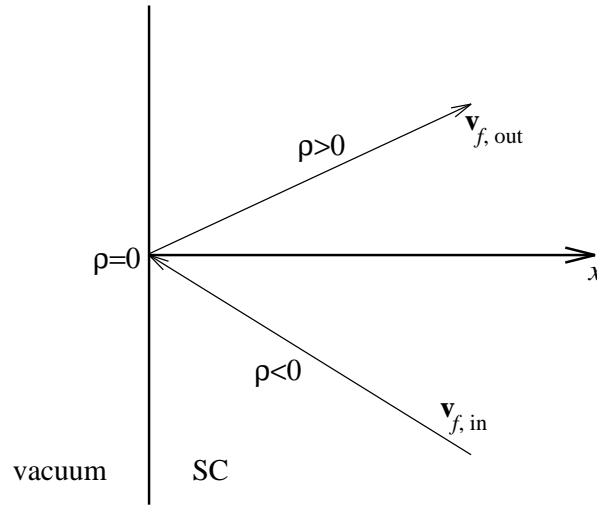


Fig. 3. A typical quasiparticle trajectory reflecting from a specular wall in the tight-binding model discussed in section II-B. The in-coming leg of the trajectory is indicated by a negative value for the trajectory parameter, ρ , with the point of reflection being at $\rho = 0$. Note that for an anisotropic Fermi surface the out-going angle is not, in general, equal to the in-coming angle.

In Fig. 4 we show some representative curves for the superconducting DOS factor (defined in equation (5)) at $x = 0$, together with profiles of the order parameter along the corresponding “trajectories” (i.e. the trajectory of a classical particle approaching the surface with velocity $\mathbf{v}_f(\mathbf{p}_{f,in})$ and leaving with velocity $\mathbf{v}_f(\mathbf{p}_{f,out})$). These curves were calculated for the case of a cylindrical Fermi surface with an order parameter of the form $\Delta \sim k_x^2 - k_y^2$. A negative value for the trajectory parameter ρ corresponds to the in-coming segment of the trajectory, while the point $\rho = 0$ corresponds to the point of reflection (a typical trajectory is depicted in Fig. 3). Note that a characteristic “edge” appears in the superconducting DOS factor corresponding to the *magnitudes* of the asymptotic values of the order parameter at $\rho = \pm\infty$. For the $\phi = 0$ deg and $\phi = 45$ deg trajectories, these values coincide so that we find only a single feature in each case at $\epsilon = (1/2)\Delta_{max-bulk}$ and at $\epsilon = (\sqrt{3}/2)\Delta_{max-bulk}$ respectively. Both the $\phi = 20$ deg and the $\phi = 45$ deg trajectories exhibit a single pole (or bound state) at $\epsilon = 0$. These states were discussed by Hu [8], and are a consequence of the Atiyah-Singer index theorem [20]. It should be emphasized that the presence of these states is a robust feature that will *always* occur (at $\epsilon = 0$) whenever the local order parameter (which is real in our gauge) changes sign asymptotically along a trajectory. The additional pole found just below the continuum in the $\phi = 0$ deg curve, on the other hand, can be interpreted as a bound state in the “potential well” formed by the order parameter along the $\phi = 0$ deg trajectory. This is not a robust feature, and will only occur if the well has sufficient depth and sufficient width. The location and weight of this feature therefore contain information on both the magnitude and the width of the order parameter suppression near the surface, which are, in turn, directly related to the degree of anisotropy in the gap.

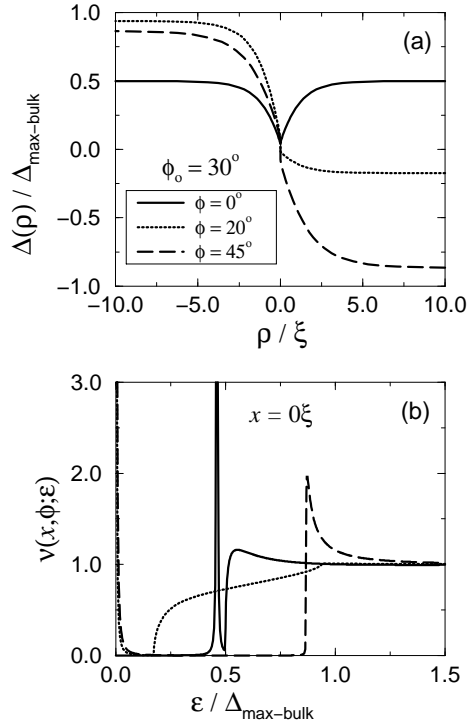


Fig. 4. Order parameter and density of states in a semi-infinite system (cylindrical Fermi surface, B_1 -symmetry): (a) the local order parameter for various (out-going) trajectory angles, ϕ , and (b) the superconducting density of states for the same trajectory angles. The lattice to surface orientation is taken to be $\phi_o = 30$ deg, and the temperature is $T = 0.4T_c$.

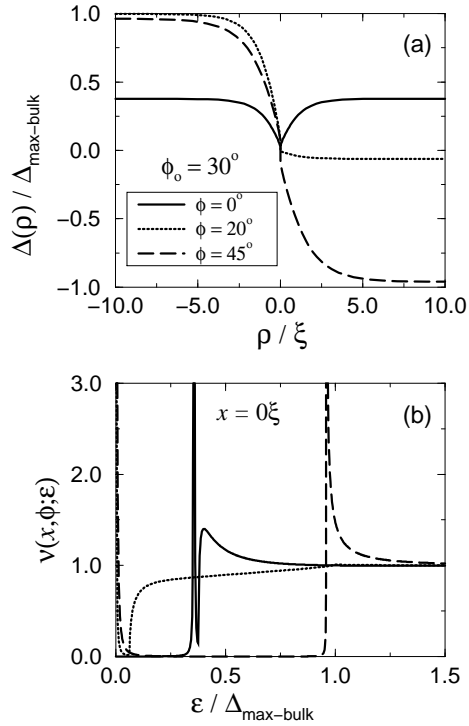


Fig. 5. Order parameter and density of states in a semi-infinite system (tight-binding Fermi surface, B_1 -symmetry): (a) the local order parameter for various (out-going) trajectory angles, ϕ , and (b) the superconducting density of states for the same trajectory angles. The lattice to surface orientation is taken to be $\phi_o = 30$ deg, and the temperature is $T = 0.4T_c$.

For essentially all surface to lattice orientations, the inclusion of nontrivial band-structure data results in rather minor effects on the density of states. In Fig. 5 we show the superconducting DOS factor for the same parameter set as in Fig. 4, only now we consider the band-structure data and pairing interaction discussed in section II-B. We have suppressed the presence of the attractive A_2 symmetry channel by artificially setting its transition temperature to zero; thus Fig. 5 corresponds to a B_1 -symmetry order parameter with a momentum dependence of the form given in Fig. 2a. Other than a redistribution of the location of the gap features, Fig. 5 is remarkably similar to Fig. 4. The fact that the gap features reorganize in this case is understandable from Fig. 2a where we see that the magnitude of the order parameter for most momentum angles has been slightly altered. However, the key point is that for a single-band Fermi surface of the form discussed in section II-B, we expect fairly little alteration in the results from the simple cylindrical Fermi surface model. Such Fermi surfaces have recently been obtained in connection with many of the high- T_c systems through the use of 2-dimensional tight-binding models [18], and therefore may be considered as reasonable models for the band-structure in some of the cuprate systems.

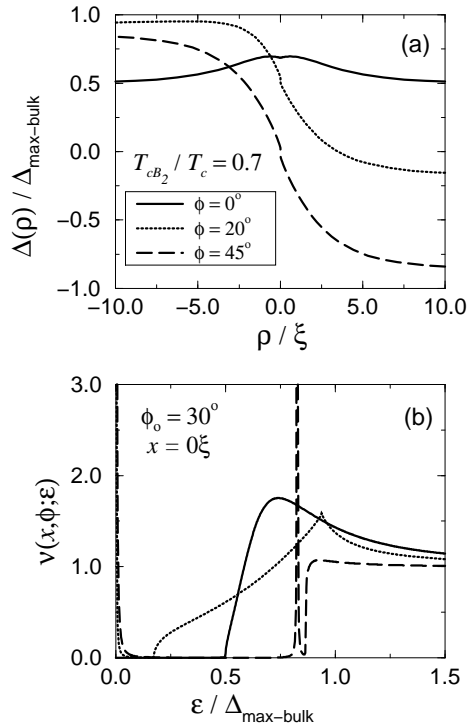


Fig. 6. Order parameter and density of states in a semi-infinite system (cylindrical Fermi surface, $B_1 + B_2$ -symmetry): (a) the local order parameter for various (out-going) trajectory angles, ϕ , and (b) the superconducting density of states for the same trajectory angles. The lattice to surface orientation is taken to be $\phi_o = 30$ deg, and the temperature is $T = 0.4T_c$.

We have also made an extensive study on the effect of the mixing of sub-dominant symmetry components with the stable bulk (B_1 -symmetry) phase. We define a sub-dominant symmetry component as any attractive symmetry channel which has a lower transition temperature than the bulk symmetry channel. These effects were discussed in detail in [I] in connection with the calculation of the self-consistent order parameter and free energy. It was shown there that the most prominent effect comes from the mixing in of the B_2 symmetry component since it allows for an effective rotation of the total order parameter towards its optimal (symmetric) configuration at the wall. This has a very pronounced *qualitative* effect on the structure of the order parameter near the wall, which is in turn discernible in the density of states. In Fig. 6 we plot the superconducting DOS factor, ν , for a system consisting of a B_1 bulk phase coupled to a B_2 symmetry component with a lower T_c . The choice of parameters is the same as in Fig. 4 for the purpose of comparison. The zero energy bound states are still present in the $\phi = 20$ deg and $\phi = 45$ deg curves since the formation of these states depends only on the asymptotic values of $\Delta(\rho)$ which are not changed when surface mixing is present (i.e. the bulk phase is not changed). The pole in the $\phi = 0$ deg trajectory, however, has now vanished since the rotation of the total order parameter gives rise to a local maximum in the order parameter near the wall rather than a local minimum. On the other hand, an additional bound state now appears just below the continuum

in the $\phi = 45$ deg curve. The appearance of this pole is a result of the broadening of the local minimum formed by the absolute value of the order parameter along the $\phi = 45$ deg trajectory when mixing is allowed to take place.

So far our discussion of the tunneling density of states has focused on the value of the superconducting DOS factor, ν , at the wall, since this is the case which is presumably accessible to tunneling experiments. For completeness, however, we show in Fig. 7 the behavior of ν as we move into the sample. Here we have selected the $\phi = 45$ deg trajectory curve from Fig. 6 since it contains both bound state features. As we move away from the wall, ν approaches its bulk form by continuously transferring weight from the bound states to the gap edge. The inset in Fig. 7 depicts the manner in which the bound state weights decay as we move into the bulk. While the zero-energy bound state is highly localized near to the wall, the upper bound state is spread out over a much broader region, which once again emphasizes the distinct nature of these two states. The ripples that develop in the superconducting DOS factor for $\epsilon > \Delta_{max-bulk}$ are Tomasch oscillations [21,22] whose prominence is a consequence of the cleanliness of our system.

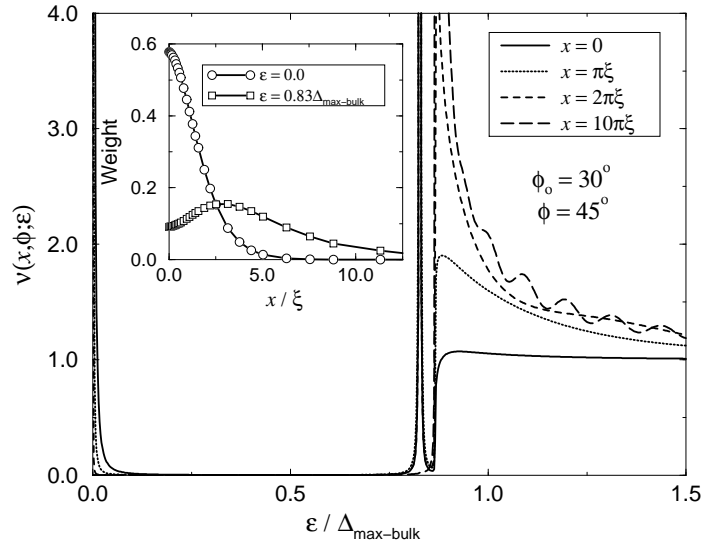


Fig. 7. The density of states for a B_1 -symmetry order parameter coupled to a sub-dominant B_2 -symmetry component as a function of distance from the wall. The inset shows the dependence on x of the weight of the two bound state delta functions (at $\epsilon = 0.0$ and at $\epsilon = 0.83$).

The mixing in of an order parameter component transforming according to the A_2 symmetry channel has also been considered. However, since the inclusion of an A_2 component only allows for a *distortion* of the B_1 order parameter in momentum space (rather than an overall *rotation*), we find very little variation in the qualitative features of the density of states.

We presented in this section our results for the angle-resolved density of states near a surface. We close this section by discussing the I-V characteristic for quasiparticle tunneling of an S-N junction where S refers to a d -wave superconductor. The differential tunneling conductance, dI/dV , is, at zero temperature, given by the following equation [23]:

$$\frac{dI}{dV} = \frac{1}{R_N} \int_{-\pi/2}^{\pi/2} d\phi D(\phi) \nu(\phi, eV), \quad (17)$$

where $\nu(\phi, eV)$ is the normalized density of states (see equation (4)), and $D(\phi)$ is the “barrier function” which is normalized such that

$$\int_{-\pi/2}^{\pi/2} d\phi D(\phi) = 1. \quad (18)$$

The function $D(\phi)$ describes the physical properties of the tunneling barrier, and therefore depends on the details of the experimental configuration. For example, a $D(\phi) = \delta(\phi)$ describes a “thick” barrier with dominant tunneling into the forward direction. Whereas a $D(\phi) = 1/\pi$ corresponds to a “random” barrier with equal probabilities of tunneling into all directions.

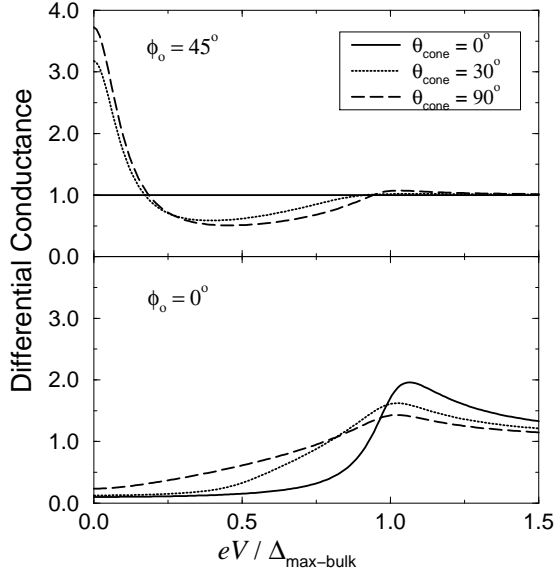


Fig. 8. The $T = 0$ differential tunneling conductance as a function of bias voltage, eV , for a (110) surface and a (100) surface and three different sampling-cone sizes. An energy width ($\sim 0.1\Delta_{\text{max-bulk}}$) has been included to simulate experimental broadening.

We present results for three types of model barriers. The barriers are described by a constant scattering probability into a “sampling cone” about the normal direction with an opening angle θ_{cone} . Specifically, we consider: (1) a thick barrier with $\theta_{\text{cone}} = 0$ deg, (2) a random barrier with $\theta_{\text{cone}} = 90$ deg, and (3) an intermediate barrier with $\theta_{\text{cone}} = 30$ deg. In Fig. 8 we show the differential tunneling conductance for these three barrier models considering the two most natural surface to lattice orientations, i.e. a [100] surface ($\phi_o = 0$ deg) and a [110] surface ($\phi_o = 45$ deg). Note that for $\phi_o = 45$ deg one finds a considerable zero-bias anomaly [8,9], while for $\phi_o = 0$ deg one finds the bulk density of states averaged over the sampling cone. Thus one expects, for d -wave superconductors with ideal surfaces, a very different tunneling characteristic depending on surface orientation. We know of no experiment which has considered the tunneling spectrum as a function of surface orientation and which would therefore be in a position to either verify or refute these clear predictions of the d -wave model.

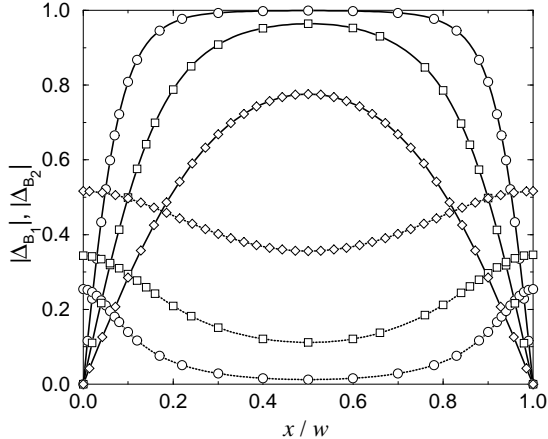


Fig. 9. Typical order parameter profiles in the slab geometry when both a B_1 and a B_2 component are present. The data are for the (1,1,0) surface ($\phi_o = 45$ deg) of the slab. The solid (dotted) lines correspond to the amplitudes of the B_1 (B_2) components. The curves are drawn for three different slab widths: $10\pi\xi$ (circles), $5\pi\xi$ (squares), and $3.5\pi\xi$ (diamonds).

B. Finite Slab

We consider a slab of finite thickness, w , and infinite lateral extent, with two specular walls located at $x = 0$ and $x = w$. This is a very convenient setting for studying surface effects since a quasiparticle experiences the surface regions several times along its trajectory. This enhances the effects of surfaces on the density of states. This system was studied in detail by Nagato *et. al.* [11] for the case of a single-component B_2 -symmetry order parameter, and a surface to lattice tilt angle of $\phi_o = 0$ deg. They discussed the existence of a phase transition from the superconducting state to the normal state as a function of layer thickness. This scenario becomes more complicated, however, if we allow the mixing-in of sub-dominant symmetry components. In this case we find, for certain tilt angles ϕ_o , that a phase transition involving only one of the symmetry components can occur, leaving the system in a superconducting state of a different symmetry. In this way the normal state is not realized until one reaches much smaller sample sizes, if at all.

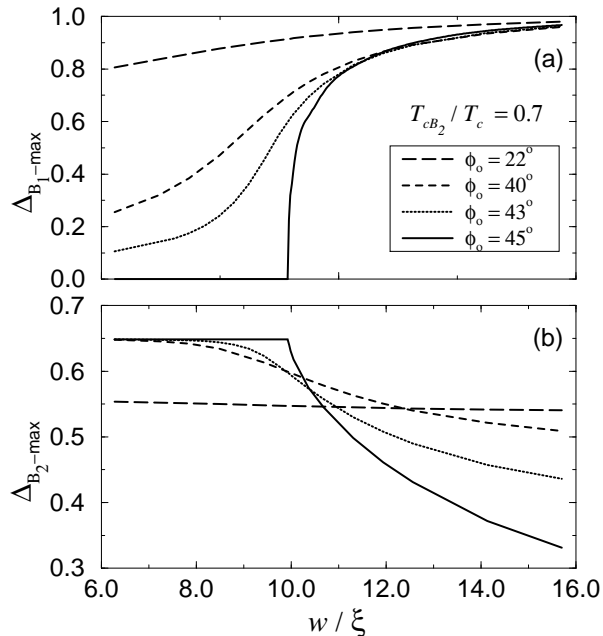


Fig. 10. The dependence of the order parameter components on the width of the slab: (a) The maximum of the B_1 -symmetry component for various slab to lattice tilt angles, ϕ_o , and (b) the maximum of the B_2 -symmetry component for the same tilt angles. Note that the system has a phase transition at a slab width $w = 9.9\xi$ for $\phi_o = 45$ deg.

In order to exhibit these effects we consider the case of an isotropic cylindrical Fermi surface and compute the self-consistent order parameter in the same manner as discussed in [1]. We again assume that the B_1 symmetry channel possesses the highest transition temperature, and allow for the mixing in of a B_2 symmetry component with $T_{cB_2}/T_c = 0.7$. In Fig. 9 we plot a typical set of order parameter profiles for a surface to lattice orientation of $\phi_o = 45$ deg and various slab widths. As the sample becomes thinner the B_1 component is strongly suppressed, while the presence of the B_2 component becomes enhanced. A plot of the maximum absolute value of each of the components as a function of the slab width is shown in Fig. 10 for several surface to lattice orientations. The angle $\phi_o = 45$ deg is a special case since it represents the maximal pair-breaking orientation for the B_1 component and the minimal pair-breaking (i.e. symmetric) orientation for the B_2 component. Hence, the B_1 component is favored in the bulk since it possesses the highest T_c , however the B_2 component is favored at the wall for symmetry reasons. As a result, at a width $w \approx 9.9\xi$ we find a second order phase transition in which the B_1 component abruptly vanishes leaving behind a spatially uniform B_2 -symmetry order parameter. As we move to angles away from $\phi_o = 45$ deg, we find that the phase transition is smeared out.

In Fig. 11 we plot the superconducting DOS factor, ν , in the vicinity of the phase transition for two different quasiparticle trajectories. The dotted lines show the form of ν below the critical width and are just what one expects for a spatially uniform order parameter (i.e. they are identical to the bulk results). Above the critical width the spectrum exhibits a complicated band-like structure [11]. Since we are considering a clean system with specular walls,

a quasiparticle will propagate without dissipation, reflecting an infinite number of times, always with the same angle of incidence. The local order parameter along such a trajectory has a periodic structure so that this scenario closely parallels the case of a particle in a periodic potential. The splitting of the excitation spectrum into bands is thus a consequence of Bloch's theorem.

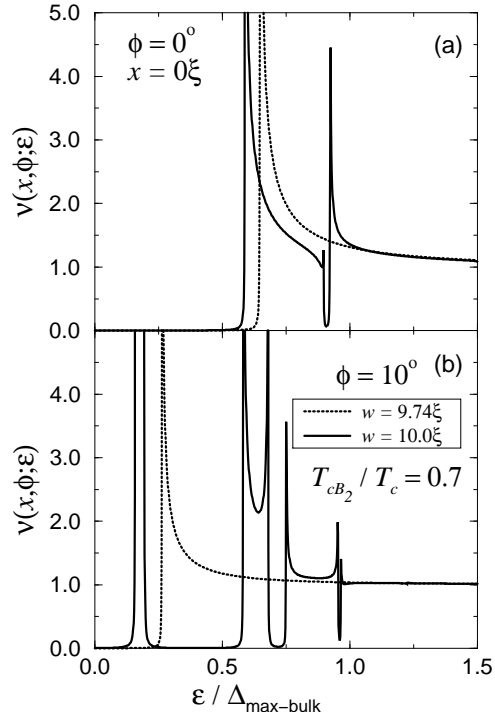


Fig. 11. The superconducting density of states in a slab with a slab to lattice orientation $\phi_o = 45$ deg. Results are shown slightly above ($w = 10.0\xi$) and below ($w = 9.7\xi$) the phase transition for two different trajectories: (a) $\phi = 0$ deg, and (b) $\phi = 10$ deg.

We have also considered the case of a B_1 -symmetry order parameter coupled to a sub-dominant A_2 -symmetry component. In this case it is the tilt angle $\phi_o = 22.5$ deg which is special, since it represents the symmetric orientation for the A_2 component. Reminiscent of the previous case, we again observe a phase transition around $w \sim 5.5\xi$ in which the B_1 component vanishes while the A_2 component becomes spatially uniform. However, here the transition is first order and, moreover, several distinct near-by metastable states compete. In the transition region, the differences in free energy between the various states are so small that specific perturbations in any experimental configuration would surely be decisive. The superconducting DOS factor, ν , exhibits distinguishing features on either side of the transition which, again, just parallels the previous case.

IV. CONCLUSIONS

We have studied the spectral properties of an anisotropically paired superconductor in the vicinity of a superconductor-insulator interface by considering two different physical geometries: a semi-infinite system, and a slab of finite width and infinite lateral extent. The stable bulk phase of the order parameter is always taken to transform like the B_1 ($d_{x^2-y^2}$) representation of the D_{4h} (tetragonal) group, however other attractive symmetry channels are also allowed to be present, which has a pronounced effect on the order parameter's behavior near the walls. The calculation of the self-consistent order parameter for systems such as these was discussed by the current authors in Ref. [13] and, we have carried over those results as input into the current calculations. All of our calculations were performed considering both an isotropic cylindrical Fermi surface, as well as a more realistic tight-binding Fermi surface; we find very little difference in the qualitative features of our results between the two Fermi surface models.

The spectra at the surface of a semi-infinite system exhibit three characteristic features. First, one finds band-edge singularities at energies corresponding to the bulk gap magnitudes $|\Delta_{bulk}(\mathbf{p}_{f,in})|$ and $|\Delta_{bulk}(\mathbf{p}_{f,out})|$ which yield

information about the gap anisotropy far from the wall. Secondly, one observes the formation of surface bound states which are of two distinct types. For any order parameter which changes its sign along the Fermi surface (regardless of its symmetry), one can always find situations in which a bound state will be formed at zero energy [8,20]. The formation of these states depends only on the relative sign of the asymptotic order parameter values ($\Delta_{bulk}(\mathbf{p}_{f,in})$ and $\Delta_{bulk}(\mathbf{p}_{f,out})$) along a quasiparticle trajectory. As a consequence, the mixing-in of sub-dominant symmetry components with the bulk (B_1) symmetry component has no impact on the presence of these states, since the order parameter is only altered within a few coherence lengths of the surface. Depending on the detailed nature of the interaction of the order parameter with the wall, however, a second species of bound states may appear at higher energies, if the order parameter is sufficiently suppressed in the surface region. The weight and location (in energy) of these bound states is directly related to the spatial dependence of the order parameter near the wall. Thus, one finds that the formation of these states can be correlated to both the strength and symmetry of the sub-dominant components. All of these features depend strongly on the surface to lattice orientation, and thus one can conceive of mapping out the full anisotropy of the order parameter by measuring the surface density of states for various surface orientations.

The study of a d -wave order parameter in a slab geometry can be especially illuminating since the percentage of the sample volume which lies in the surface region is significantly enhanced. For the case of single d -wave order parameter in a finite slab, one finds phase transitions for certain surface to lattice orientations which results in a nontrivial temperature vs. width phase diagram [11]. When the bulk B_1 symmetry order parameter is allowed to couple to a B_2 symmetry component, these phase transitions are washed out for most surface orientations. For certain “special” surface orientations however, phase transitions still occur (of either first or second order) which may take the sample into the normal state or even into a state with a different bulk symmetry. These special orientations are usually those in which the sub-dominant component does *not* pair-break. These phase transitions have a pronounced effect on the excitation spectrum since the order parameter always has a complicated spatial structure on one side of the transition while it is completely structureless on the other.

The calculations presented in this paper were carried out for clean superconductors with perfectly reflecting surfaces. This is important to note because the presence of a diffuse boundary could result in significant qualitative effects. Indeed, our ongoing work indicates that for diffuse surfaces the distinction between the various surface to lattice orientations may no longer be as clear, since any one in-coming trajectory may mix with all out-going trajectories. This effect tends to smear-out, to variable degrees, some of the aforementioned phase transitions and characteristic features in the surface excitation spectrum. We conclude that a concerted effort should be made to fabricate “clean” surfaces, with specific surface to lattice orientations, if the maximal quantity of information on the anisotropy of the order parameter and the surface induced features in the density of states is to be extracted.

ACKNOWLEDGEMENTS

The research of L.J.B was supported by the Fulbright Commission and that of M.P. by the Alexander von Humboldt-Stiftung. D.R. was supported, in part, by the Graduiertenkolleg “Materialien und Phänomene bei sehr tiefen Temperaturen” of the DFG. J.A.S. acknowledges partial support by the Science and Technology Center for Superconductivity through NSF Grant no. 91-20000. Authors D.R. and J.A.S. also acknowledge additional support from the Max-Planck-Gesellschaft and the Alexander von Humboldt-Stiftung.

-
- [1] L. J. Buchholtz and G. Zwirnagl, Phys. Rev. B **23**, 5788 (1981).
 - [2] W. Zhang, J. Kurkijärvi, and E. Thuneberg, Phys. Lett. **109A**, 238 (1985).
 - [3] J. Hara and K. Nagai, Prog. Theor. Phys. **76**, 1237 (1986).
 - [4] W. Zhang, J. Kurkijärvi, and E. Thuneberg, Phys. Rev. B **36**, 1987 (1987).
 - [5] T. Tokuyasu, J. A. Sauls, and D. Rainer, Phys. Rev. B **38**, 8823 (1988).
 - [6] L. J. Buchholtz, Phys. Rev. B **44**, 4610 (1991).
 - [7] N. B. Kopnin, P. I. Soininen, and M. Salomaa, J. Low Temp. Phys. **85**, 267 (1991).
 - [8] C.-R. Hu, Phys. Rev. Lett. **72**, 1526 (1994).
 - [9] S. Kashiwaya and Y. Tanaka, Phys. Rev. B **51**, 1350 (1995).
 - [10] Y. Tanaka and S. Kashiwaya, Phys. Rev. Lett. **74**, 3451 (1995).
 - [11] Y. Nagato and K. Nagai, Phys. Rev. B **51**, 16254 (1995).
 - [12] M. Matsumoto and H. Shiba, J. Phys. Soc. Jpn. **64**, 1703 (1995).
 - [13] L. J. Buchholtz, M. Palumbo, D. Rainer, and J. A. Sauls, J. Low Temp. Phys. **101**, (1995).
 - [14] J. W. Serene and D. Rainer, Physics Reports **4**, 221 (1983).
 - [15] Y. N. Ovchinnikov, Zh. Eksp. Teor. Fiz. **56**, 1590 (1969).
 - [16] J. Kurkijärvi, D. Rainer, and J. Sauls, Can. J. Phys. **65**, 1440 (1987).
 - [17] R. J. Radtke, S. Ullah, K. Levin, and M. R. Norman, Phys. Rev. B **46**, 11975 (1992).
 - [18] R. J. Radtke and M. R. Norman, Phys. Rev. B **50**, 9554 (1994).
 - [19] M. R. Norman, private communication (1995).
 - [20] M. F. Atiyah, V. K. Patodi, and I. M. Singer, Proc. Camb. Phil. Soc. **77**, 43 (1975).
 - [21] W. J. Tomasch, Phys. Rev. Lett. **15**, 672 (1965).
 - [22] W. J. Tomasch, Phys. Rev. Lett. **16**, 16 (1966).
 - [23] C. B. Duke, *Tunneling in Solids*, 1 ed. (Academic Press, New York, 1969), Chap. 7.